A novel guidance law design for gap traversal of unmanned aerial vehicles

Kumar Abhinav

***Abstract*— This paper proposes a novel guidance law that allows unmanned aerial vehicles to traverse through gaps. The proposed approach employs a barrier Lyapunov function framework that leverages the gap bearing information to ensure successful traversal. The guidance law is formulated for scenarios where the gap information is available a priori but can also be adapted for situations where gap edge detection depends on active vision techniques. Notably, the design operates within a nonlinear framework without linearizing any system dynamics, allowing it to remain effective even when the states significantly deviate from their nominal values. The effectiveness of the proposed guidance law is evaluated through detailed numerical simulations. These results validate the efficacy of the proposed guidance law design for the gap traversal of aerial vehicles.**

Barrier Lyapunov function, Guidance law design, Unmanned aerial vehicle, Monte Carlo simulations

I. INTRODUCTION

Nowadays, unmanned aerial vehicles (UAV) are in high demand due to their applicability in various domains for important and interesting purposes. Nowadays, there are enormous emerging applications of UAVs to traverse a gap in a constrained environment. To avoid collisions with obstacles that may lead to catastrophic consequences, it is inevitably required to pass through narrow gaps successfully. In constrained environments, enabling multiple UAVs to transport a payload simultaneously (such as delivery cases) adds significant importance to achieving successful gap traversal. These challenging situations devise the need for successful gap traversal in the constraint environments. Gap traversal has become important in many applications as well, such as surveillance, traffic monitoring, rescue, cargo transportation, etc.

Several planning algorithms have addressed the challenge of guiding aerial vehicles through apertures in indoor settings with strict constraints. While passing through gaps, these algorithms ensure the vehicle maintains a safe distance from barriers. Mellinger et al. [1], [2] developed planning and control methods enabling quadrotors to generate smooth trajectories that navigate through stationary gaps and sequences of waypoints while minimizing snap. These approaches rely on prior knowledge of gap locations, which may not be available in real-world environments, increasing collision risk in complex settings.

The authors [3] addressed the gap traversal problem by framing it as an optimization task grounded in a predetermined collection of flight paths. Nonetheless, the reliance on manually defined parameters could restrict the exploration of more efficient solutions. Moreover, there is no conclusive proof that the constraints used in this approach consistently lead to optimal outcomes. The authors in [4] approached the problem using an optimal control framework with predefined assumptions. The approach was based on several assumptions: that the flight path would be parabolic, motor thrust would remain unchanged, the vehicle's angular velocity would be zero during traversal, and the trajectory's starting point would be predetermined. Moreover, the technique required foreknowledge of the gap.

Several investigations have developed onboard sensing methods to detect and estimate gap edges as a way to tackle this challenge. In particular, [5] and [6] employed reinforcement learning strategies for quadrotor gap traversal. Nevertheless, inaccuracies in gap detection in these studies could increase the likelihood of collisions in real-world scenarios. The authors [7] used active vision techniques for gap traversal, leveraging an onboard single-camera sensor to detect edges and guide navigation. Despite their promise, these reinforcement learning-based methods rely on training and testing cycles, where the learned policies may not adequately address unmodeled dynamics.

The bearing-only measurement (BOM) algorithm allows for a reduction in the number of sensors required for UAV navigation tasks, thus lowering the overall system cost [8]. Moreover, BOM-based algorithms are particularly advantageous in radio-silent operations [8]. Bearings can be acquired through image sensors [9], eliminating the need for signal transmission during UAV maneuvers. The study [10] investigated the application of barrier Lyapunov function (BLF) to ensure state-constrained motion in nonlinear systems. Similarly, BLF in combination with sliding mode control was explored in [11]. Impact angle control guidance with a seeker's field-of-view constraint, utilizing BLF, was introduced in [12]. The guidance strategies based on the Bearing-Only Measurement (BOM) were explored for mobile agents operating in a two-dimensional environment [13], [14]. These methods leveraged bearing vectors and subtended angles measured from three fixed beacons to guide the agents to their desired positions. Extensive research has focused on developing guidance laws [15]–[17]. These studies encompass a variety of techniques, including classical proportional navigation and its improved variants, robust sliding mode control strategies, and approaches for controlling impact angle and impact time.

Many existing gap traversal methods, including those described in [2], [3], utilize multi-phase controller archi-

*Kumar Abhinav is with the Department of Aerospace Engineering, IIT Bombay, Maharashtra, India, 214010016@iitb.ac.in

tectures, which tend to impose significant computational demands on the system. Several cost-effective methods that leverage bearing-based control strategies were proposed [18]–[21]. In these methods, the quadrotor first aligns itself with the midpoint before advancing toward the gap. By contrast, our method enables the quadrotor to directly pursue a path toward the gap, thereby reducing traversal time.

This paper proposes a novel barrier Lyapunov function-based guidance approach for gap traversal by aerial vehicles. The proposed guidance law capitalizes on bearing information, specifically the line-of-sight (LOS) angle and range, to enable efficient gap traversal. The primary contributions of this work can be summarized as follows:

- The proposed guidance law is solely based on bearing angle and range measurements. This bearing-only measurement approach decreases the number of sensors needed for navigation, enhancing cost-effectiveness.
- The guidance law is formulated within a nonlinear framework without linearization, allowing it to remain applicable even with significant deviations in the flight path and heading angles.
- To the best of our knowledge, the proposed guidance law design is versatile and applicable to various aerial vehicles.

II. Problem formulation

This section presents the formulation of the problem that serves as the foundation for the proposed guidance law design. The gap can be considered a stationary target, enabling the application of missile guidance theories to facilitate effective gap traversal. Consequently, we begin by analyzing the relative motion dynamics between the vehicle and the gap to establish a guidance law that ensures safe traversal. These relative motion dynamics will then serve as the basis for the guidance law design in the following section.

Assumption 1: The bearing information of the gap, acquired through visual sensors, is assumed to be known.

Assumption 2: The gap size is considerably large relative to the size of the vehicle, allowing for the assumption of wider gap traversal.

This study examines how the proposed design enables successful gap traversal in a planar environment. The comprehensive investigation into the interaction between the vehicle and the gap in two-dimensional space is presented in Fig. 1. It is also worth mentioning that this approach can be similarly applied to scenarios in the longitudinal plane.

Let us introduce fundamental parameters necessary to comprehend the vehicle's interaction with the gap. The velocity of the vehicle, symbolized as v_m, is a key factor in facilitating the gap crossing, as illustrated in Fig. 1 for movements in the lateral direction. Moreover, the heading angle, expressed as α_v is crucial for evaluating the relative movement of the vehicle throughout the engagement process. It is assumed that the gap bearing angles and range are known, which are acquired through certain visual sensing mechanisms. To align with this assumption, the vehicle's position is given by (x, y), whereas the positions of the two

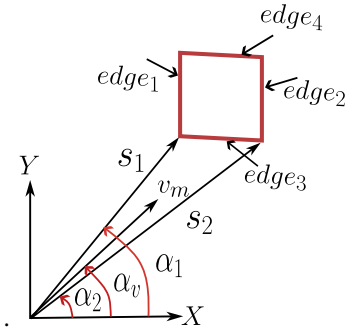

Fig. 1: Engagement geometry in the lateral plane.

gap edge corners are specified as (x_{c1}, y_{c1}) and (x_{c2}, y_{c2}), respectively, as illustrated in Fig. 1. The line-of-sight distance s_1 to the first edge of the gap, denoted as $edge_1$, can be determined using the equation below:

$$s_1 = \sqrt{(x_{c1} - x)^2 + (y_{c1} - y)^2}.$$

The bearing angle α_1 can be evaluated as follows:

$$\alpha_1 = \tan^{-1}\left[\frac{y_{c1} - y}{x_{c1} - x}\right]. \tag{1}$$

At this stage, the relative velocity can be determined as

$$v_{s_1} = -v_m \cos(\alpha_v - \alpha_1). \tag{2}$$

The range s_2 and bearing angle α_2 corresponding to gap edge 2 can be calculated in a similar fashion. The rate of change of the relative line-of-sight (LOS) angle between the vehicle and the first gap edge can be expressed as

$$s_1\dot{\alpha}_1 = -v_m \sin(\alpha_v - \alpha_1). \tag{3}$$

In a similar manner, the relative velocity between the vehicle and the second gap edge can be represented as

$$v_{s_2} = -v_m \cos(\alpha_v - \alpha_2). \tag{4}$$

The rate of variation of the line-of-sight (LOS) angle relative to the second gap edge can be defined as

$$s_2\dot{\alpha}_2 = -v_m \sin(\alpha_v - \alpha_2). \tag{5}$$

The derived relative velocities and line-of-sight (LOS) rates, informed by the gap geometry, will be employed in the next section to formulate the guidance strategies for the gap traversal.

A. Kinematic bicycle model

The proposed design is validated using the kinematic bicycle model, which serves as a simplified point-mass representation of the vehicle in a planar scenario. The vehicle is modeled using the bicycle abstraction, wherein the pair of front wheels is represented as a single equivalent front wheel, and similarly, the rear wheels are combined into one virtual rear wheel. This simplified representation assumes planar motion and neglects dynamics related to roll, pitch, and suspension. Let the term x, y denote the positions of the vehicle center of mass in the global coordinate frame and the

term v be the velocity of the vehicle. The term α_v represents the orientation of the vehicle with respect to the global X-axis. The equation of motion of the kinematic bicycle model can be expressed as

$$\dot{x} = v_m \cos(\alpha_v) \tag{6}$$

$$\dot{y} = v_m \sin(\alpha_v) \tag{7}$$

$$\dot{\alpha}_v = \frac{v_m}{L} \tan(\delta), \tag{8}$$

where the term $\tan(\delta)$ accounts for the curvature of the vehicle's path resulting from front-wheel steering and the term L denotes the wheelbase, assumed to be constant throughout the motion.

The fundamental principle of our approach is based on the assumption that any gap shape can accommodate an inscribed rectangular region, allowing the proposed method to be generalized for various gap geometries. Building on the previous discussions, the problem statement is outlined as follows:

Problem 1: To design a cost-effective guidance law for gap traversal of aerial vehicles, relying solely on the gap line-of-sight angle and range.

Remark 1: The proposed guidance law is developed within a nonlinear framework, ensuring its effectiveness even in substantial initial deviations in heading and flight path angles during gap traversal.

III. Guidance law design

This section proposes the guidance law design for the gap traversal of aerial vehicles. We introduce an auxiliary variable, $\hat{\alpha}_m$, defined as the difference between the vehicle heading angle, α_v, and the bisector of the bearing angles α_1 and α_2. To ensure that this variable stays within a desired range, a barrier Lyapunov function is employed in the design of the guidance law for gap traversal. When $\hat{\alpha}_m$ remains within its bounds, it guarantees that the heading angle α_v is situated between the bearing angles of the two gap edges, thereby ensuring that the vehicle successfully traverses through the gap. It can be formulated as

$$\hat{\alpha}_m = \alpha_v - \frac{\alpha_1 + \alpha_2}{2}. \tag{9}$$

The derivative of $\hat{\alpha}_m$ can be expressed as

$$\dot{\hat{\alpha}}_m = \dot{\alpha}_v - \frac{\dot{\alpha}_1}{2} - \frac{\dot{\alpha}_2}{2}. \tag{10}$$

Upon using the expressions for $\dot{\alpha}_1$ and $\dot{\alpha}_2$ from (3) and (5), respectively, we derive

$$\dot{\hat{\alpha}}_m = \dot{\alpha}_v + \frac{v_m}{2s_1} \sin(\alpha_v - \alpha_1) + \frac{v_m}{2s_2} \sin(\alpha_v - \alpha_2). \tag{11}$$

Now, these equations of $\hat{\alpha}_m$ can be expressed in an affine form such that guidance based on BLF can be designed. On expressing it in affine form, we have

$$\hat{\alpha}_m = u_1, \tag{12}$$

where, there is limit for $\hat{\alpha}_m$ as it varies from $-k_1 < \hat{\alpha}_m < k_1$. To facilitate this constraint on the auxiliary variable, the barrier Lyapunov function is chosen as

$$V = \frac{1}{2} \ln \frac{{k_1}^2}{{k_1}^2 - {u_1}^2}. \tag{13}$$

The derivative of the Lyapunov function with respect to time can be represented as

$$\dot{V} = \frac{u_1 \dot{u_1}}{{k_1}^2 - {u_1}^2}. \tag{14}$$

Now, $\dot{u_1}$ can be expressed as

$$\dot{V} = \frac{u_1}{{k_1}^2 - {u_1}^2} \left[\dot{\alpha}_v + \frac{v_m}{2s_1} \sin(\alpha_v - \alpha_1) + \frac{v_m}{2s_2} \sin(\alpha_v - \alpha_2) \right]. \tag{15}$$

Now, the dynamics of the kinematic bicycle model, from 8, can be substituted in 15 as

$$\dot{V} = \frac{u_1}{{k_1}^2 - {u_1}^2} \left[\frac{v_m}{L} \tan(\delta) + \frac{v_m}{2s_1} \sin(\alpha_v - \alpha_1) + \frac{v_m}{2s_2} \sin(\alpha_v - \alpha_2) \right]. \tag{16}$$

The term $\tan(\delta)$ serves as lateral control variable, therefore we have

$$\tan(\delta) = \frac{L}{v_m} \left[-\frac{v_m}{2s_1} \sin(\alpha_v - \alpha_1) - \frac{v_m}{2s_2} \sin(\alpha_v - \alpha_2) - k_2 u_1 ({k_1}^2 - {u_1}^2) \right]. \tag{17}$$

Once we define $\tan(\delta)$ as given above, the time derivative of V can consequently be expressed as

$$\dot{V} = -k_2 {u_1}^2. \tag{18}$$

This result demonstrates that, for any positive value of k_2, the barrier Lyapunov function ensures stability. Simulation outcomes are discussed in the next section.

IV. Simulation results

The planar motion of the kinematic bicycle model is showcased in this section with the proposed guidance law design. An elliptical shaping function for gap traversal was employed in the previous work by the authors in [19]. The performance of the guidance law proposed in this paper is evaluated through a comparative analysis with the method in [19]. The results are illustrated in Fig. 2 and Fig. 3. While the guidance aspect of the proposed approach is similar to the classical velocity pursuit method, it advances the velocity pursuit by incorporating a Barrier Lyapunov Function (BLF) within a bearing-based control framework. This integration allows the heading angle relative to the gap edges to be rigorously constrained during gap traversal. Consequently, a comparative analysis with the deviated pursuit approach is performed and depicted in Fig. 2 and Fig. 3.

A small step size of 0.01 is selected to ensure high accuracy, while the gap width is fixed at 5 meters. The BLF gains are set to $k_1 = 0.5$ and $k_2 = 5$. The simulation

proceeds until the vehicle has successfully passed through the gap, at which point the guidance algorithm is terminated. The first corner of the gap edge ($edge_1$) is located at $(5, 25)$ meters, while the second corner ($edge_2$) is positioned at $(10, 25)$ meters. The simulations in Fig. 2 begin with initial conditions $x(0) = 5$ and $y(0) = 10$. The initial value for $\hat{\alpha}_m$ is set to 0.1 rad. As depicted in Figure 2b, the vehicle avoids collisions with the edges and successfully passes through the gap. The position trajectories, shown in Fig. 2c, demonstrate smooth, oscillation-free motion. The velocity pursuit approach tends to bring the vehicle very close to one edge of the gap, leading to an undesirable curved trajectory near the gap, as depicted in Fig. 2c. The variations in the lateral acceleration, heading angle $\hat{\alpha}_m$ are shown in Fig 2d. Notably, the lateral acceleration remains minimal throughout, as shown in Fig 2d. The BLF gain k_1 enforces constraints that keep the vehicle's heading angle within the bearing angles of the gap, as demonstrated in Fig. 2e.

The simulations depicted in Fig. 3 utilize initial states of $x(0) = 15$ and $y(0) = 10$. From Fig. 3a, it is evident that the vehicle follows a more direct and shorter trajectory along both x and y axes compared to the method reported in [19], enabling efficient gap traversal. Additionally, as shown in Fig. 3c, the proposed approach achieves faster gap traversal. Traveling at a constant speed of 1 m/s, the vehicle reaches the gap in 16.38 seconds using our method, whereas the approach in [19] requires 17.98 seconds to cover the same distance.

The simulations presented in Fig. 4 are performed under noisy conditions, where the bearing measurements of the gap edges are assumed to be corrupted by noise. This case is modelled by adding a random variable drawn from a normal distribution $\mathcal{N}(0, 1)$ with zero mean and unit variance to the gap edge coordinates in the world frame. Such noise simulates sensor inaccuracies that can degrade edge detection quality and subsequently impact system performance. Furthermore, Monte Carlo simulations with 100 trials are conducted using different initial positions located on a circle of radius 10 m centered at the gap midpoint $(7.5, 25)$, as illustrated in Fig. 4. Despite the presence of Gaussian noise on the bearing data, the position states remain unaffected, and successful gap traversal is consistently achieved across all tested initial conditions.

Additionally, we have provided simulation results for different values of k_1 in Fig. 5, which reveal that increasing k_1 enhances the control effort required, but does not significantly alter the vehicle's position trajectory during gap traversal. Moreover, Fig. 6 illustrates successful gap traversal under varying gap dimensions using the same initial conditions, thereby highlighting the robustness and adaptability of our proposed method for a range of gap shapes.

The robustness of the proposed design is highlighted in Fig. 7, where a step disturbance of magnitude $66°$ is introduced to the LOS angle α_1. The response of the proposed guidance law is compared with that of a Lyapunov function-based guidance approach. The results demonstrate that the proposed method outperforms the latter by eliminating oscillations and enabling smooth gap traversal without abrupt changes in the trajectory. It should be noted that the initial heading angle of the vehicle must adhere to the LOS angle constraints defined by the BLF-based design to ensure reliable performance.

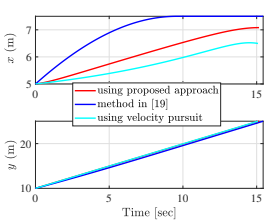

(a) Motion in xy plane.

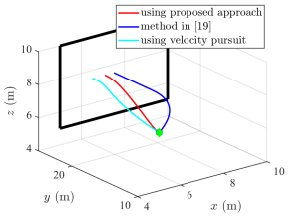

(b) Trajectory in $3D$ view.

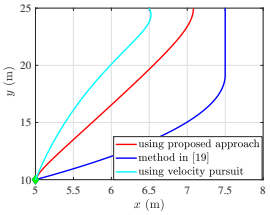

(c) Variation in positions.

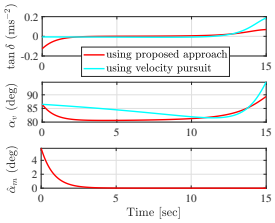

(d) Variation in control input, heading angle, and $\hat{\alpha}_m$.

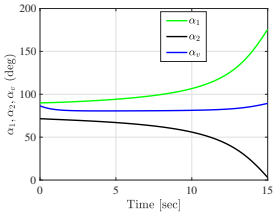

(e) Variation in bearing and heading angles.

Fig. 2: Comparison of performance for the point mass vehicle in a plane with $x(0) = 5$ and $y(0) = 10$.

V. Conclusion

This research proposed a barrier Lyapunov function based guidance law design for gap traversal of aerial vehicles. The simulation results were provided to show the effectiveness of the proposed control design based on the bearing angles of the gap, and it was shown to be efficient. The simulation results demonstrated that the proposed guidance design required minimal control demands and achieved gap traversal in a relatively short time. Future studies suggest implementing the proposed guidance design on the fixed-wing UAV platform with potential extensions to the quadrotor and other vehicles.

References

[1] D. Mellinger and V. Kumar, "Minimum snap trajectory generation and control for quadrotors," in *International Conference on Robotics and Automation*. IEEE, 2011, pp. 2520–2525.

[2] D. Mellinger, N. Michael, and V. Kumar, "Trajectory generation and control for precise aggressive maneuvers with quadrotors," *The International Journal of Robotics Research*, vol. 31, no. 5, pp. 664–674, 2012.

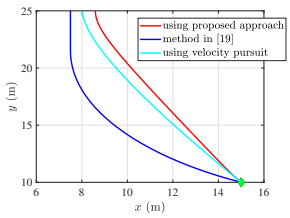

(a) Motion in xy plane.

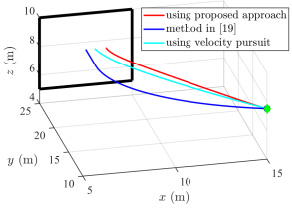

(b) Trajectory in $3D$ view.

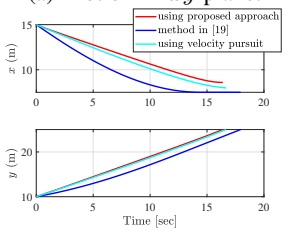

(c) Variation in positions.

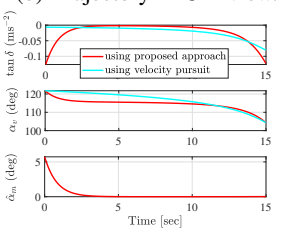

(d) Variation in control input, heading angle, and $\hat{\alpha}_m$.

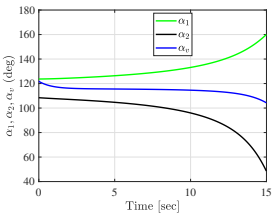

(e) Variation in bearing and heading angles.

Fig. 3: Comparison of performance for the point mass vehicle in a plane with $x(0) = 15$ and $y(0) = 10$.

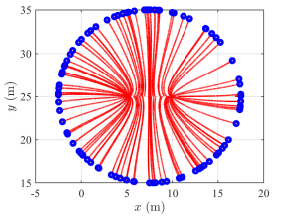

(a) xy planar view.

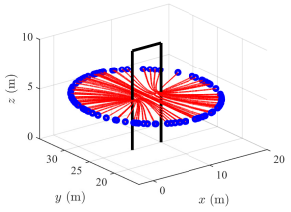

(b) $3D$ view.

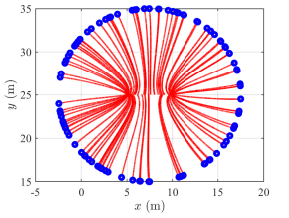

(c) xy planar view with Gaussian noise.

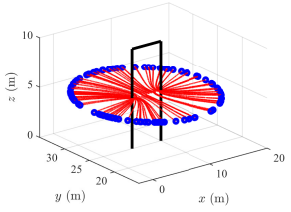

(d) $3D$ view with Gaussian noise.

Fig. 4: Monte Carlo simulation results comparing vehicle performance with and without noise.

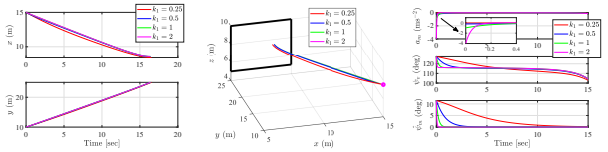

(a) Motion in xy plane.

(b) Trajectory in $3D$ view.

(c) Variation in control input, heading angle, and $\hat{\alpha}_m$.

Fig. 5: Gap traversal with different values of k_1.

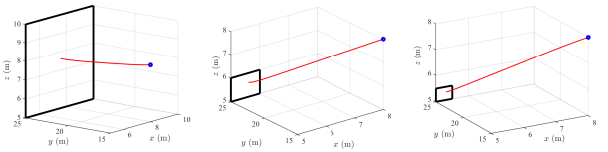

(a) Gap: 500×500 cm

(b) Gap: 100×100 cm

(c) Gap: 50×50 cm

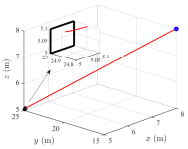

(d) Gap: 10×10 cm

Fig. 6: Gap traversal with $x(0) = 8$, $y(0) = 15$, $z(0) = 8$

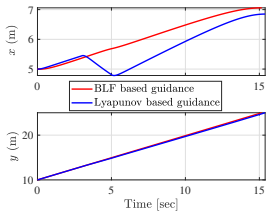

(a) Variation in positions.

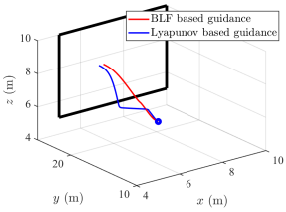

(b) Trajectory in $3D$.

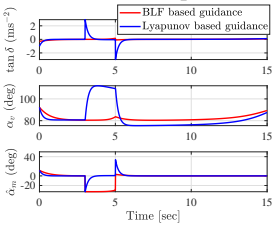

(c) Variation in control input, heading angle, and $\hat{\alpha}_m$.

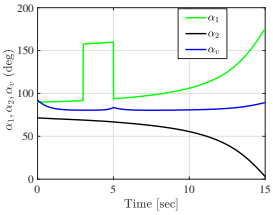

(d) LOS and heading angles.

Fig. 7: Gap traversal in the presence of disturbance.

[3] D. Falanga, E. Mueggler, M. Faessler, and D. Scaramuzza, "Aggressive quadrotor flight through narrow gaps with onboard sensing and computing using active vision," in *IEEE International Conference on Robotics and Automation*. IEEE, 2017, pp. 5774–5781.

[4] G. Loianno, C. Brunner, G. McGrath, and V. Kumar, "Estimation, control, and planning for aggressive flight with a small quadrotor with a single camera and imu," *IEEE Robotics and Automation Letters*, vol. 2, no. 2, pp. 404–411, 2016.

[5] S. Chen, Y. Li, Y. Lou, K. Lin, and X. Wu, "Learning real-time dynamic responsive gap-traversing policy for quadrotors with safety-aware exploration," *IEEE Transactions on Intelligent Vehicles*, vol. 8, no. 3, pp. 2271–2284, 2022.

[6] C. Xiao, P. Lu, and Q. He, "Flying through a narrow gap using end-to-end deep reinforcement learning augmented with curriculum learning and sim2real," *IEEE Transactions on Neural Networks and Learning Systems*, vol. 34, no. 5, pp. 2701–2708, 2021.

[7] Y. Xie, M. Lu, R. Peng, and P. Lu, "Learning agile flights through narrow gaps with varying angles using onboard sensing," *IEEE Robotics and Automation Letters*, 2023.

[8] M. Deghat, L. Xia, B. D. Anderson, and Y. Hong, "Multi-target localization and circumnavigation by a single agent using bearing mea-

surements," *International Journal of Robust and Nonlinear Control*, vol. 25, no. 14, pp. 2362–2374, 2015.

[9] H. Choi and Y. Kim, "Uav guidance using a monocular-vision sensor for aerial target tracking," *Control Engineering Practice*, vol. 22, pp. 10–19, 2014.

[10] K. P. Tee, B. Ren, and S. S. Ge, "Control of nonlinear systems with time-varying output constraints," *Automatica*, vol. 47, no. 11, pp. 2511–2516, 2011.

[11] D. Cruz-Ortiz, I. Chairez, and A. Poznyak, "Sliding-mode control of full-state constraint nonlinear systems: A barrier lyapunov function approach," *IEEE Transactions on Systems, Man, and Cybernetics: Systems*, vol. 52, no. 10, pp. 6593–6606, 2022.

[12] S. Zhou, S. Zhang, and D. Wang, "Impact angle control guidance law with seeker's field-of-view constraint based on logarithm barrier lyapunov function," *IEEE Access*, vol. 8, pp. 68 268–68 279, 2020.

[13] M. H. Trinh, K.-K. Oh, and H.-S. Ahn, "Control of a mobile agent using only bearing measurements in triangular region," in *Seventh IEEE Symposium on Computational Intelligence for Security and Defense Applications*. IEEE, 2014, pp. 1–5.

[14] M. H. Trinh, G.-H. Ko, V. H. Pham, K.-K. Oh, and H.-S. Ahn, "Guidance using bearing-only measurements with three beacons in the plane," *Control Engineering Practice*, vol. 51, pp. 81–91, 2016.

[15] B. S. Kim, J. G. Lee, and H. S. Han, "Biased png law for impact with angular constraint," *IEEE Transactions on Aerospace and Electronic Systems*, vol. 34, no. 1, pp. 277–288, 1998.

[16] A. Manjunath, P. Mehrok, R. Sharma, and A. Ratnoo, "Application of virtual target based guidance laws to path following of a quadrotor uav," in *International Conference on Unmanned Aircraft Systems*. IEEE, 2016, pp. 252–260.

[17] B.-G. Park, T.-H. Kim, and M.-J. Tahk, "Optimal impact angle control guidance law considering the seeker's field-of-view limits," *Proceedings of the Institution of Mechanical Engineers, Part G: Journal of Aerospace Engineering*, vol. 227, no. 8, pp. 1347–1364, 2013.

[18] E. Midhun and A. Ratnoo, "Safe traversal guidance for quadrotors using gap bearing information," in *International Conference on Unmanned Aircraft Systems*. IEEE, 2021, pp. 482–487.

[19] ——, "Gap traversal guidance using bearing information," *Journal of Guidance, Control, and Dynamics*, vol. 45, no. 12, pp. 2360–2368, 2022.

[20] ——, "Bearing information-based trajectory planning for window traversal," in *International Conference on Control, Decision and Information Technologies*. IEEE, 2023, pp. 1291–1295.

[21] A. Ratnoo *et al.*, "Quadrotor guidance for window traversal: A bearings-only approach," *arXiv preprint arXiv:2410.14367*, 2024.